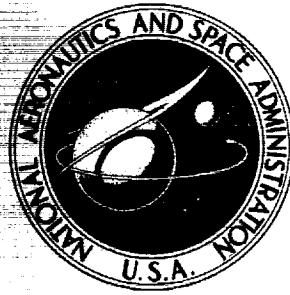


**NASA TECHNICAL
MEMORANDUM**



NASA TM X-2120

NASA TM X-2120

**CASE FILE
COPY**

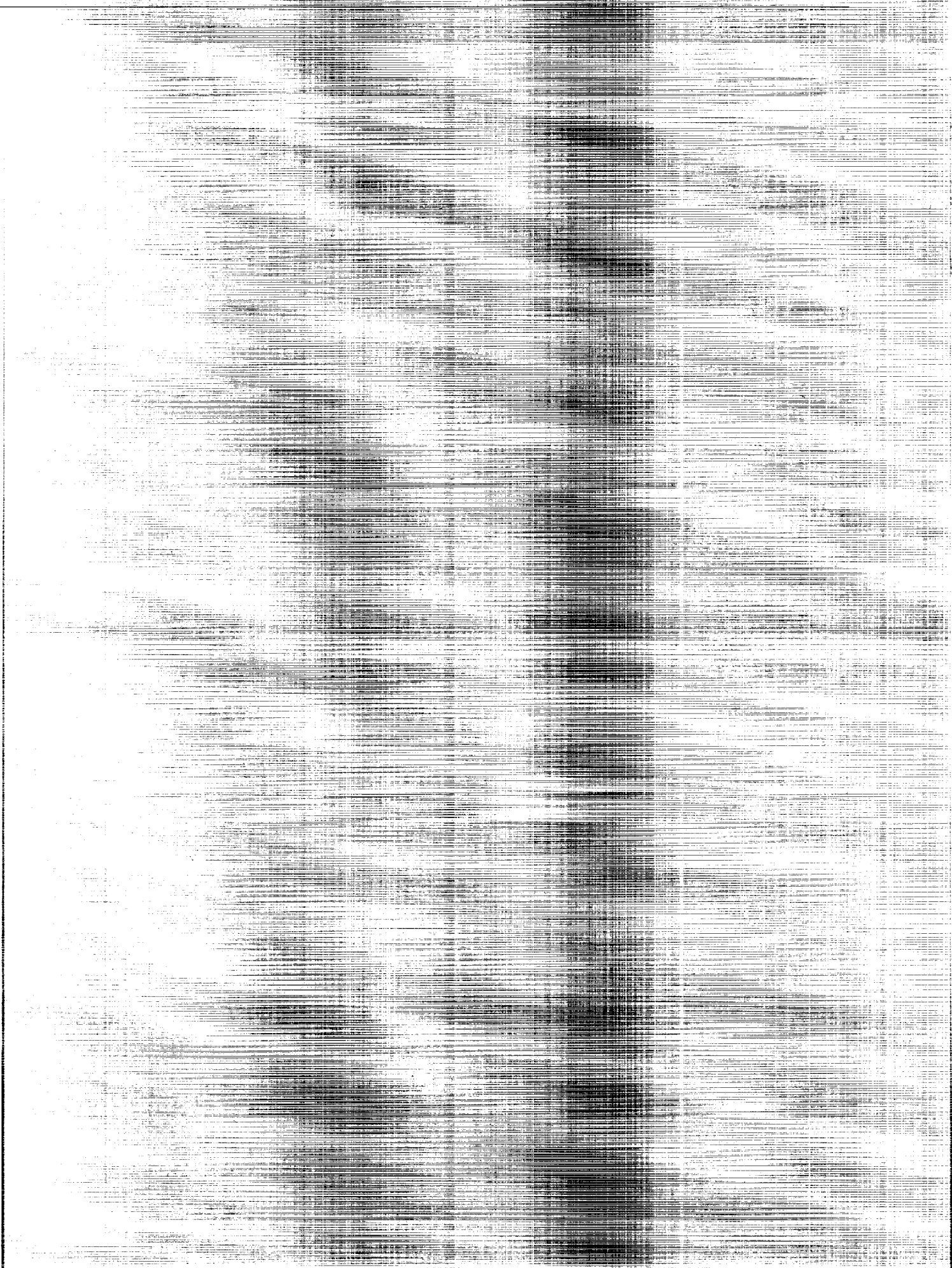
**SOME OBSERVATIONS OF EFFECTS OF
POROUS CASINGS ON OPERATING RANGE OF
A SINGLE AXIAL-FLOW COMPRESSOR ROTOR**

by Everett E. Bailey and Charles H. Voit

Lewis Research Center

Cleveland, Ohio 44135

NATIONAL AERONAUTICS AND SPACE ADMINISTRATION • WASHINGTON, D. C. • OCTOBER 1970



| | | | |
|---|---|--|-----------------------------|
| 1. Report No. NASA TM X-2120 | 2. Government Accession No. | 3. Recipient's Catalog No. | |
| 4. Title and Subtitle SOME OBSERVATIONS OF EFFECTS OF POROUS CASINGS ON OPERATING RANGE OF A SINGLE AXIAL-FLOW COMPRESSOR ROTOR | | 5. Report Date October 1970 | |
| | | 6. Performing Organization Code | |
| 7. Author(s) Everett E. Bailey and Charles H. Voit | | 8. Performing Organization Report No. E-5695 | |
| | | 10. Work Unit No. 720-03 | |
| 9. Performing Organization Name and Address Lewis Research Center National Aeronautics and Space Administration Cleveland, Ohio 44135 | | 11. Contract or Grant No. | |
| | | 13. Type of Report and Period Covered Technical Memorandum | |
| 12. Sponsoring Agency Name and Address National Aeronautics and Space Administration Washington, D. C. 20546 | | 14. Sponsoring Agency Code | |
| | | 15. Supplementary Notes | |
| 16. Abstract The results of testing a single axial-flow rotor with several porous outer casings are presented. Comparative tests were made with tip radial inlet flow distortion. An improvement in the stable operating range of the rotor was noted for some of the porous casing configurations. Some loss in rotor performance was noted when a porous casing was present. | | | |
| 17. Key Words (Suggested by Author(s)) Compressor casing treatment Compressor operating range improvement | | 18. Distribution Statement Unclassified - unlimited | |
| 19. Security Classif. (of this report) Unclassified | 20. Security Classif. (of this page) Unclassified | 21. No. of Pages 30 | 22. Price* \$3.00 |

*For sale by the Clearinghouse for Federal Scientific and Technical Information
Springfield, Virginia 22151

CONTENTS

| | Page |
|--|------|
| SUMMARY | 1 |
| INTRODUCTION | 2 |
| APPARATUS | 3 |
| Test Rotor | 3 |
| Porous Casings | 5 |
| Tapered holes | 5 |
| Honeycomb | 5 |
| Radial drilled holes | 5 |
| Instrumentation | 9 |
| Distortion Screens. | 10 |
| RESULTS AND DISCUSSION | 11 |
| Solid Wall Casing | 11 |
| Uniform inlet flow. | 11 |
| Radial inlet flow distortion | 16 |
| Porous Casings - Comparative Tests. | 16 |
| Tapered holes - configurations 2 to 6 | 18 |
| Honeycomb - configurations 7 to 12 | 20 |
| Radial drilled holes - configurations 13 and 14 | 22 |
| Tests with Uniform Inlet Flow and Circumferential Distortion | 23 |
| Uniform inlet flow. | 23 |
| Circumferential inlet flow distortion. | 24 |
| CONCLUDING REMARKS | 25 |
| APPENDIX - TABULATION OF OVERALL PERFORMANCE DATA | 27 |
| REFERENCES | 28 |

|

SOME OBSERVATIONS OF EFFECTS OF POROUS CASINGS ON OPERATING RANGE OF A SINGLE AXIAL-FLOW COMPRESSOR ROTOR

by Everett E. Bailey and Charles H. Voit

Lewis Research Center

SUMMARY

A single axial-flow compressor rotor was tested with a solid wall casing and with several porous casings over the rotor tip. This report presents experimental comparisons of the effectiveness of the porous casings to permit operation of the rotor to lower flows before rotating stall was observed (i. e. , to improve the stall limit). Basic porous casing configurations included tapered holes set at a compound angle, honeycomb with passages inclined at a 70° angle to the radial direction, and radial drilled holes. These porous casings were surrounded by a plenum. The recirculatory flows between the plenum and the main airstream through the passages were varied by means of bands and baffles. The comparative tests were made with tip radial inlet flow distortion.

Results indicate that both tapered holes and honeycomb can be instrumental in obtaining a substantial stall limit improvement. The amount of the improvement was approximately the same for these two basically different porous casing configurations. Some observations related to the particular basic configurations are

(1) For the tapered-hole configuration, recirculation appeared to be a necessity for stall limit improvement, and the amount of the improvement was directly related to the recirculation.

(2) With the honeycomb configuration, it appeared that the stall limit improvement was derived from different mechanisms than that for the tapered holes.

(3) With the honeycomb configuration and uniform inlet flow, a loss in rotor pressure ratio and efficiency occurred in the tip region.

(4) The plenum volume around the honeycomb could be made quite small with no change in the stall limit improvement. However, when the plenum volume was zero, no improvement was obtained.

INTRODUCTION

Present and future applications of jet engines for aircraft propulsion have indicated a need for increased stable operating flow range of the axial-flow compressors and fans used. This is particularly significant for those engines which utilize advanced compressor and fan design concepts such as increased stage loading and/or high-aspect-ratio blading. In order to realize the maximum benefit, the increase in flow range should be in the operating region between maximum compressor or fan efficiency and the low flow stability limit. For many fans and compressors, this low flow stability limit is the onset of rotating stall. Thus some means of delaying rotating stall and allowing the fan or compressor to operate to lower flows would be desirable.

During an evaluation of the effects of blowing or bleeding through the outer casing in the vicinity of the rotor tip, it was noted that the presence of the porous casing yielded a significant improvement in the rotor stall limit when no blowing or bleeding flow was used. This improvement was with respect to the stall limit noted for the rotor with a solid wall casing built under NASA contract, the results of which are reported in reference 1. The improvement was most pronounced when either a tip radial or a 90° circumferential inlet flow distortion was present. This was attributed to the fact that the tip was critical (i. e. , rotating stall was first noted in the tip region) with these flow conditions. With uniform inlet flow, the rotating stall for this particular rotor appeared to initiate in the midspan region rather than at the blade tip. Thus, for those conditions where the blade was tip critical, the porous casing over the rotor tip permitted operation at lower overall weight flows for a given speed than were possible with a solid wall casing.

The aerodynamic phenomena, or flow mechanisms, associated with the presence of the porous casing were not readily identifiable or detectable. The phenomena discussed in this report are recirculation, circumferential variation in static pressure, and acoustical tuning. The porous casing surrounded by a plenum presents paths for recirculation over the rotor blade tip. If a stall cell forms in a rotor, a circumferential variation in static pressure must exist around the rotor. The porous casing plus plenum may permit the equalization of this static pressure and therefore delay the formation of a rotating stall cell. Also, for any one point on the outer wall, the static pressure is pulsating with respect to time at the blade passing frequency. Thus, there may be some acoustical relation associated with the interchange of pressure and flows between the main air-stream and the plenum.

Additional tests were conducted by the General Electric Company under a second NASA contract utilizing the hardware from reference 1 with some modifications. This second program was for the purpose of obtaining additional information regarding the potential gain in stall margin which might be obtained from porous casings. Compara-

tive tests of various configurations were made with tip radial inlet flow distortion. From these, one configuration was selected and tested with uniform inlet flow and with a 90° circumferential inlet flow distortion.

This report presents the following results from the second program: (1) overall performance of the solid wall casing configuration with uniform inlet and tip radial distortion; (2) comparisons of the stall limit lines obtained for the several porous casing configurations to that for the solid wall casing when operated with tip radial distortion; (3) for the one selected porous casing configuration operated with uniform inlet flow, a comparison of the stability limit to the stall limit obtained with the solid wall casing, and a comparison of the design speed efficiencies to that for the solid wall casing; (4) for this same selected porous casing configuration, a comparison of the stall limit line to that obtained for the solid wall casing when both were operated with circumferential inlet flow distortion; (5) a tabulation of the overall performance data taken during this program; and (6) some observations regarding operation of particular configurations, which should be an aid to further studies regarding the use of porous casings as a means of obtaining improved stall limits.

APPARATUS

Test Rotor

The rotor aerodynamic and mechanical design is described in detail in reference 2. Design parameters of this high-aspect-ratio, transonic, compressor rotor are

| | |
|---|-------|
| Rotor tip speed, ft/sec | 1120 |
| Inlet hub-tip radius ratio | 0.50 |
| Total pressure ratio, radially constant | 1.47 |
| Weight flow, lb/sec | 187 |
| Weight flow per unit annulus area, lb/(sec)(ft ²) | 39.32 |
| Rotor tip diameter, in. | 34 |
| Rotor tip solidity | 1.0 |
| Rotor tip relative Mach number | 1.2 |
| Rotor tip diffusion factor | 0.45 |
| Rotor blade aspect ratio | 4.5 |
| Rotor blade chord, radially constant, in. | 1.77 |
| Number of rotor blades | 60 |

and the rotor blade section is a double circular-arc on cylindrical sections. A segment of the rotor is shown in figure 1. The outer and inner contours of the flow path in the

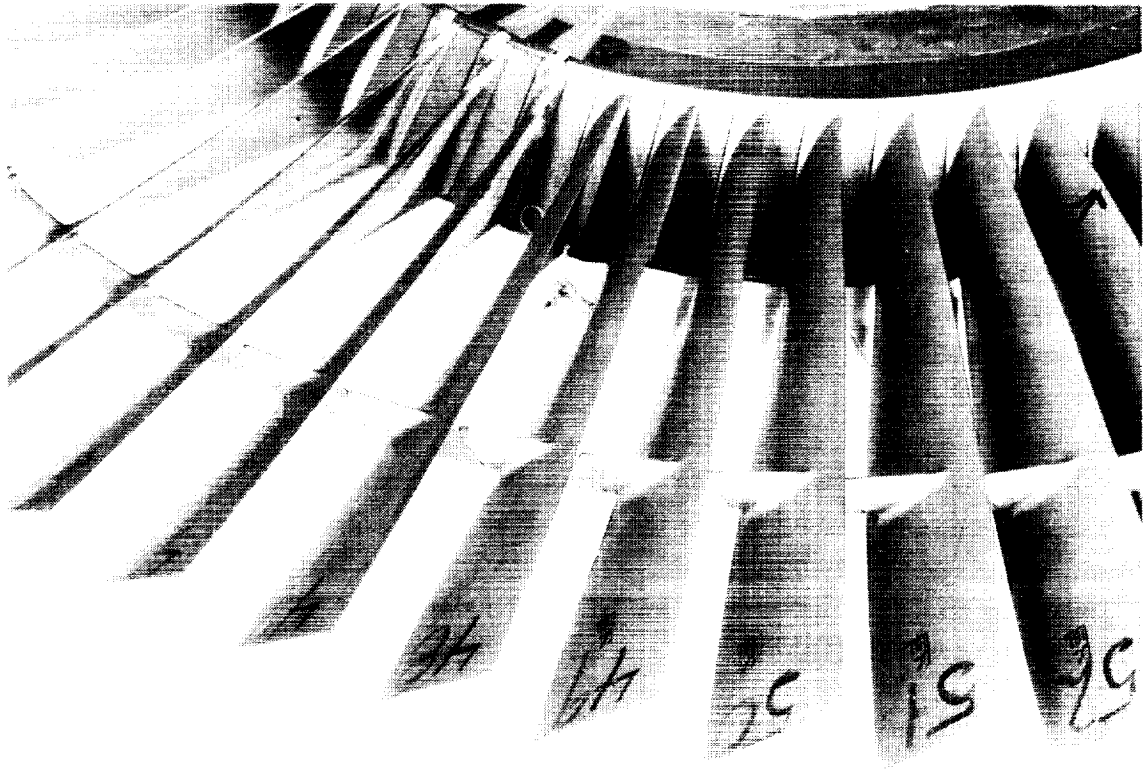


Figure 1. - Segment of test rotor.

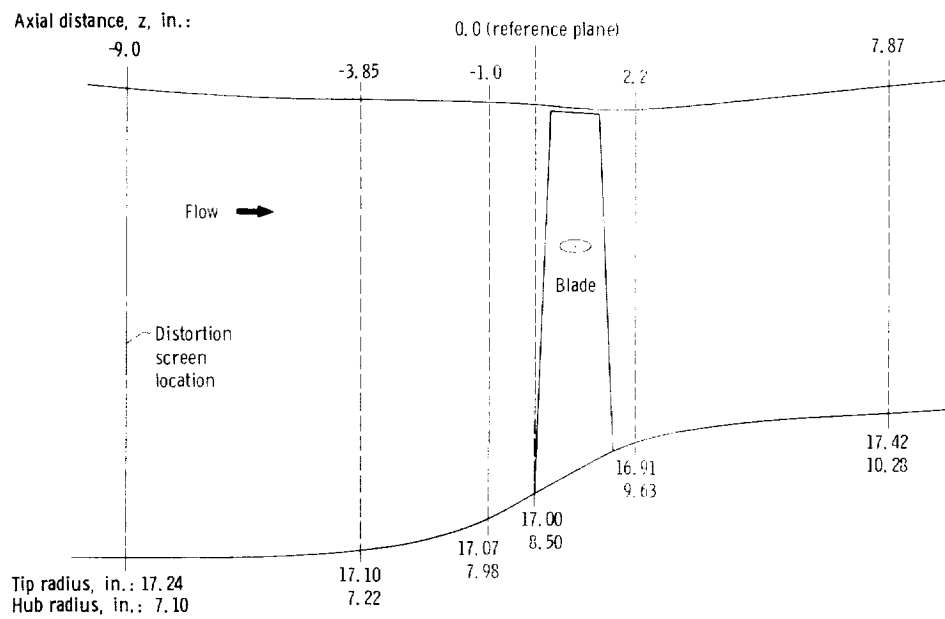


Figure 2. - Flow path and instrumentation locations.

vicinity of the rotor are shown in figure 2. Outlet guide vanes for removal of the swirl were located approximately $13\frac{1}{2}$ inches downstream from the reference location shown on figure 2. The General Electric Company test facility had an atmospheric inlet and discharge.

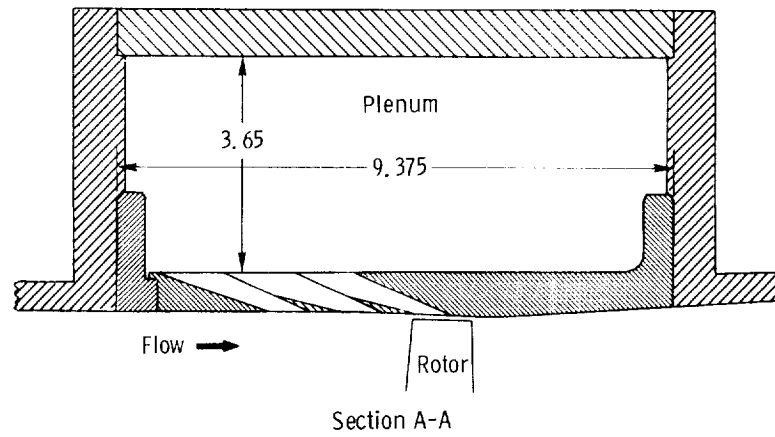
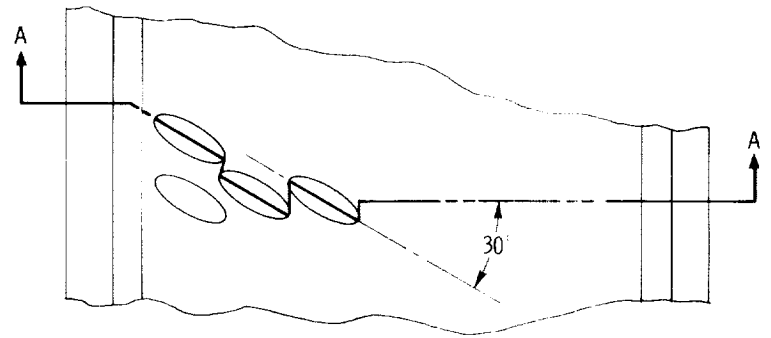
Porous Casings

The porous casing configurations are separated into three groupings according to the type of opening through the casing: (1) tapered holes, (2) honeycomb, and (3) straight radial drilled holes. The basic configurations designed as interchangeable casing inserts are described below and in figures 3 to 5. Various modifications to the basic configurations are identified and shown by sketches in table I (p. 13). In the figures and sketches, the relation of the holes, honeycomb, and so forth, to the rotor blade tip shown are approximately to scale.

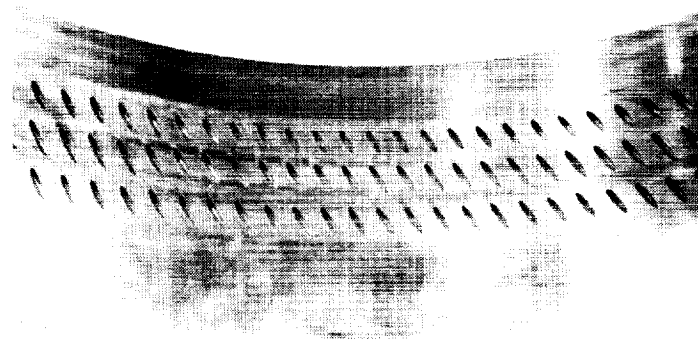
Tapered holes. - The insert shown in figures 3(a) and (b) contained three rows of tapered holes set at a compound angle. One row of holes pierced the inside of the casing over the rotor blade tip and the other two rows were forward of the rotor blade tip. Each row contained 116 holes. The centerline of each hole formed a 70° angle with the radial direction and a 30° angle with the axial direction. This orientation is such that air emitting from the small end of the tapered hole into the main stream would be directed downstream and opposite to rotor rotation. The minimum diameter of the holes was 0.25 inch. This is blowing insert configuration 1 of reference 3. Configurations 2 to 6 utilize this insert.

Honeycomb. - The insert shown in figures 4(a) and (b) contained a stainless-steel honeycomb segment mounted over and ahead of the rotor blade tip. The centerline of the honeycomb passages formed a 70° angle with the radial direction and a 90° angle with the axial direction. The inclination from the radial is in the direction of rotor rotation (see section A-A of fig. 4). This is bleed insert configuration 3 of reference 2. The material which originally filled the honeycomb passages ahead of the rotor blade tip region was removed for this program. Configurations 7 to 12 utilize this insert.

Radial drilled holes. - This insert was obtained by drilling 0.25-inch diameter holes in the solid wall casing. Details of the hole locations and pattern are shown in figure 5. Configuration 13 contained two rows of holes over the rotor tip. Configuration 14 contained two additional rows ahead of the rotor tip. Each row contained 200 holes equally spaced on approximately 0.5-inch centers.

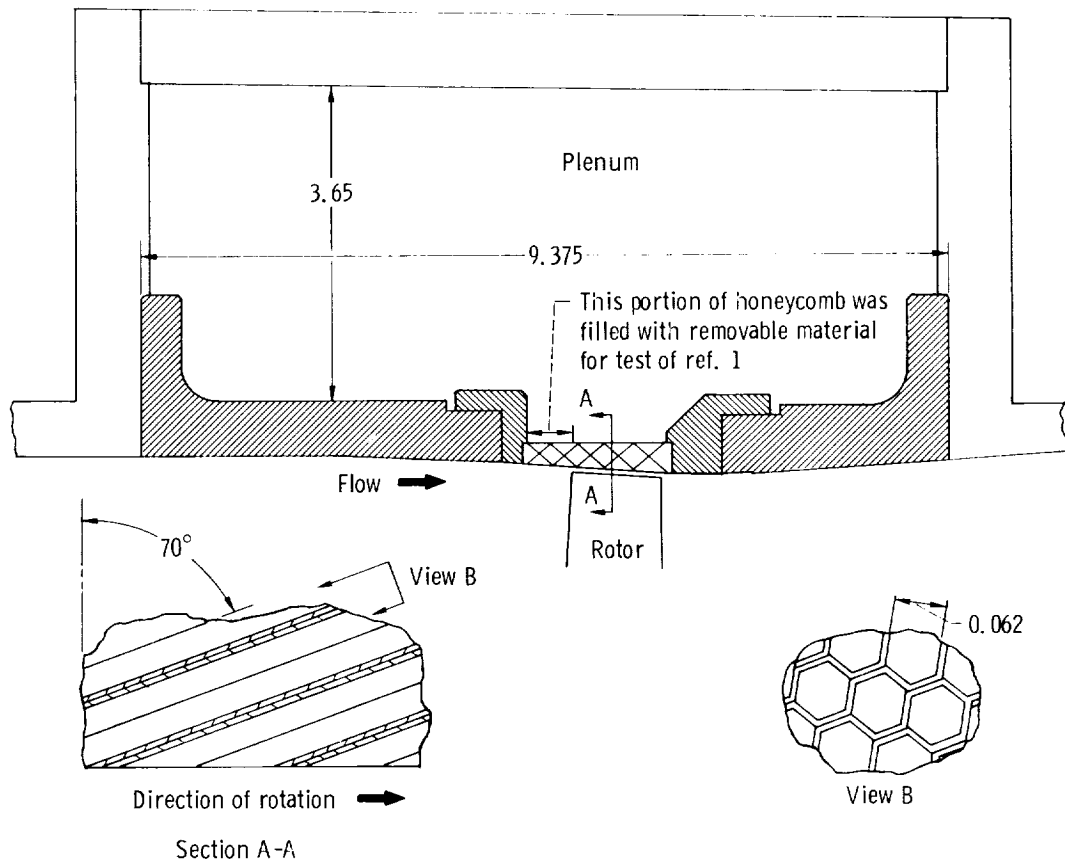


(a) Sketch showing hole orientation and location.

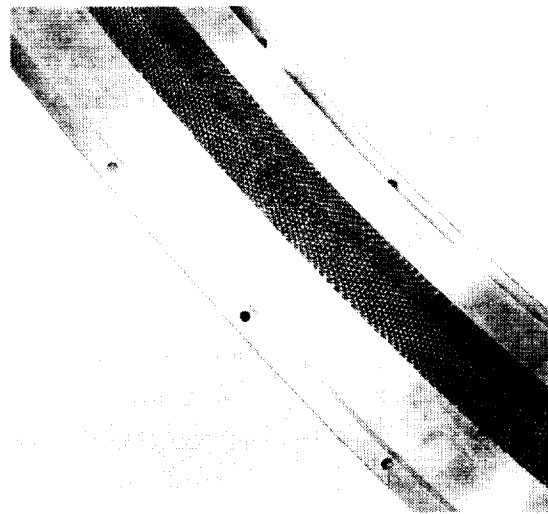


(b) Inside of tapered-hole casing.

Figure 3. - Tapered-hole porous casing. (Dimensions are in inches.)



(a) Sketch showing honeycomb orientation and location.



(b) Inside of honeycomb casing.

Figure 4. - Honeycomb porous casing. (Dimensions are in inches.)

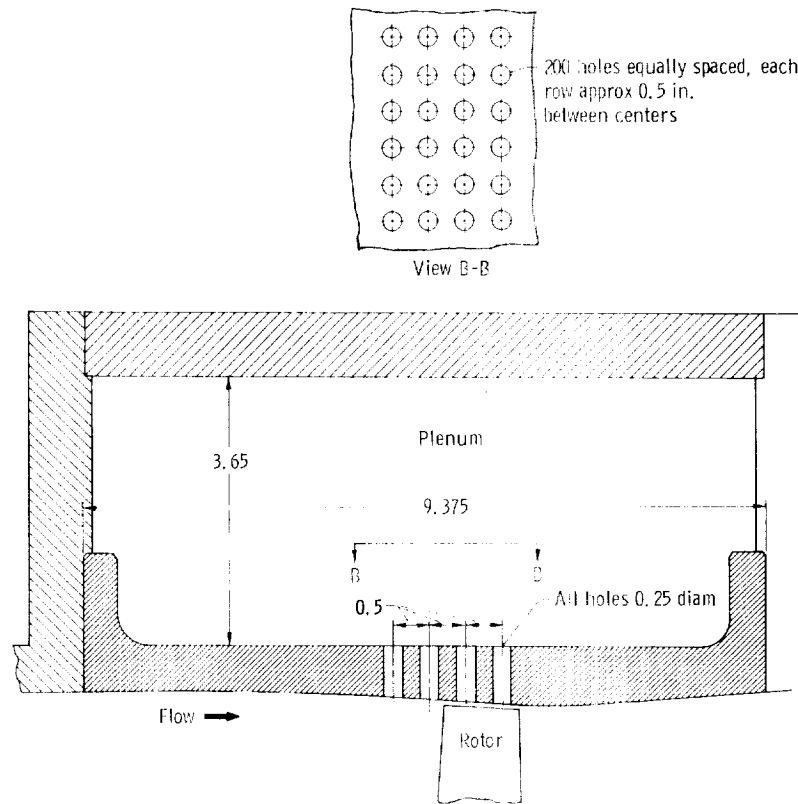


Figure 5. - Radial-drilled-hole porous casing. (Dimensions are in inches.)

Instrumentation

The axial locations of the instrumentation pertinent to this report are shown on figure 2. These are dimensioned from a reference plane which intersects the leading edge of the rotor blade at the hub. Inlet total pressure was obtained from four multiple-tube rakes 3.85 inches ahead of the reference plane at circumferential locations of 16° , 106° , 196° , and 286° (increasing in the direction of rotor rotation). Measurements were obtained at radii corresponding to 10, 30, 50, 70, and 90 percent of span. Outlet total pressure was obtained from similar-type rakes 7.87 inches downstream from the reference plane (see fig. 2). Measurements were obtained at 10, 30, 50, 70, and 90 percent of span. The circumferential locations of the rakes were 17° , 107° , 185° , and 275° .

Inlet temperature was measured in a low-velocity region ahead of the compressor. Outlet total temperature was obtained from four multiple-element rakes at the same axial location and percent of span as the outlet total pressure. The circumferential locations of the rakes were 5° , 95° , 197° , and 287° . Wall static pressures were measured at the outer casing 1.0 inch ahead of the reference plane and 2.2 inches down-

stream from the reference plane. Airflow was measured by means of a calibrated venturi flowmeter located in each of the three exhaust pipes. Weight flow at the stall limit was measured in the bellmouth ahead of the rotor. These measurements were correlated with the metered flow values at the steady-state points. Rotor speed was measured by an electronic counter. Rotating stall was detected by hot-wire probes located at the axial station 2.2 inches downstream from the reference plane. Photographs of the instrument rakes and the hot-wire probes are presented in references 3 and 4.

Distortion Screens

The screens for both radial and circumferential distortion were mounted about 9 inches upstream of the rotor (fig. 2). The radial distortion screen covered the outer 40 percent of the inlet annulus area and the circumferential screen covered the lower 90° arc of the annulus, as shown in figure 6. Both screens were supported by a coarse

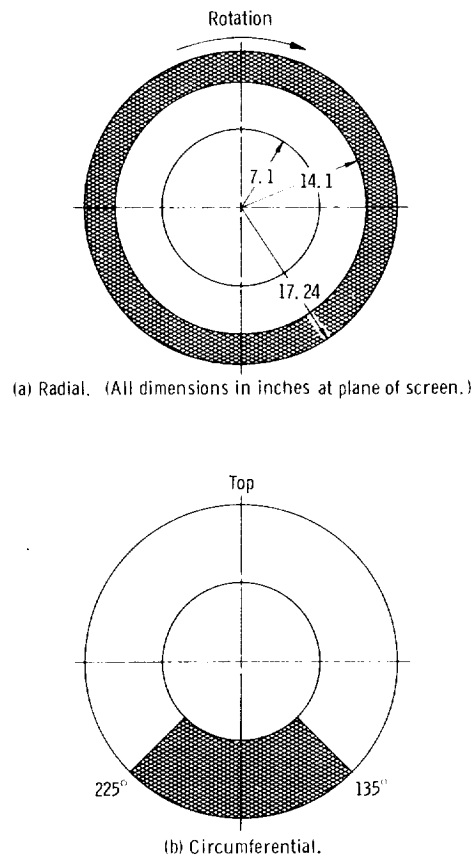


Figure 6. - Extent and location of distortion screens (looking forward).

screen having a 0.092-inch wire diameter with 0.75-inch spacing. The radial distortion screen was 16 mesh and 0.018-inch wire diameter. This gave a measured value of maximum total pressure minus minimum total pressure divided by maximum total pressure $(P_{\max} - P_{\min})/P_{\max}$ of approximately 0.16 at the measuring station 3.85 inches ahead of the rotor when operating with a flow of 184 pounds per second. The circumferential screen was the same as that described in references 3 and 4 with 20 mesh and 0.016-inch wire diameter. This screen gave a $(P_{\max} - P_{\min})/P_{\max}$ of approximately 0.20 at a flow of 174 pounds per second.

RESULTS AND DISCUSSION

The results presented herein are based primarily on the overall performance obtained from the fixed rake instrumentation described in the section APPARATUS. A tabulation of the overall performance data for each combination of configuration and inlet flow condition tested is given in table II (see appendix). Further information concerning these data is given in the appendix. Information will be drawn from table II for discussion in the following order: First, the overall performance with the solid wall casing is shown for both uniform inlet flow and tip radial inlet flow distortion. These establish a base line or reference for comparison of the effects of porous casings. Secondly, the stall limit line obtained with each porous casing configuration operated with tip radial distortion is compared to that of the base line. Similar comparisons between certain porous casing configurations are also made. Finally, from these comparisons, one porous casing configuration was selected and tested with uniform inlet flow and circumferential inlet flow distortion. These results are compared to the base line in terms of (1) the location of the stall or stability limit line; and (2) for the uniform inlet condition, the design speed efficiencies.

Solid Wall Casing

Uniform inlet flow. - The overall performance for the subject rotor with a solid wall casing is shown in figure 7. At design speed, this rotor had a stable operating flow range of approximately 20 pounds per second and a peak efficiency of 0.89. At lower speeds, the peak efficiency was 0.92 to 0.93. Considering the high-aspect-ratio blading and the level of blade loading, the flow range and efficiencies are good. During the original testing (reported in ref. 1), it was noted that this rotor appeared not to be tip critical with uniform inlet flow; that is, the rotating stall was observed first in the midspan region rather than at the rotor tip. The vibration dampers are located in the midspan region.

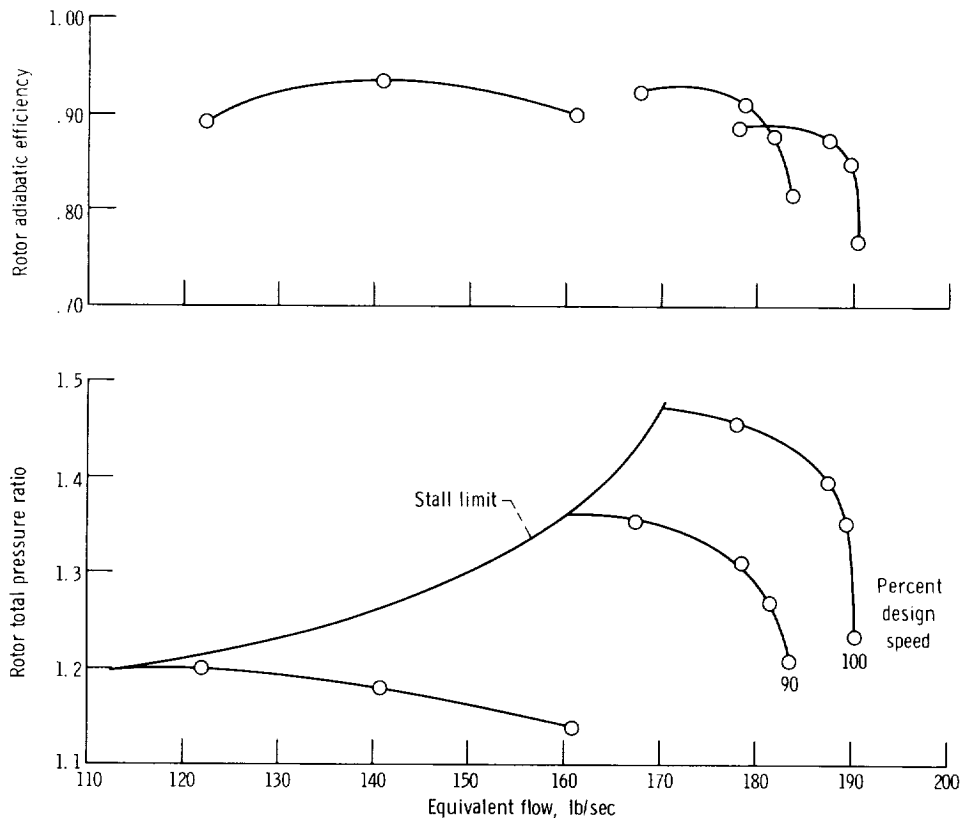


Figure 7. - Performance map for test rotor with uniform inlet flow and solid wall casing.

Radial inlet flow distortion. - The results of testing this rotor with a tip radial inlet flow distortion are shown in figure 8 with a comparison to uniform inlet flow. There was a large deterioration of stable flow range with distortion. The stall limit line for distortion is to the right and below that for uniform inlet flow. There was also a loss in overall efficiency of about 7 to 8 points at design speed. With this inlet flow condition, the rotor was definitely tip critical with the rotating stalls initiating at the tip.

Porous Casings - Comparative Tests

The effects of a porous casing over the rotor tip on stable operating range should be more easily detected for a rotor which is tip critical. Thus, the comparative tests, discussed in this section, were run with a tip radial inlet flow distortion. With radial inlet flow distortion, the overall rotor efficiency values were not used as criteria for assessing the effectiveness of porous casings. An assumption of linear variation of static pressure between hub and tip was used in mass weighting the discharge total tem-

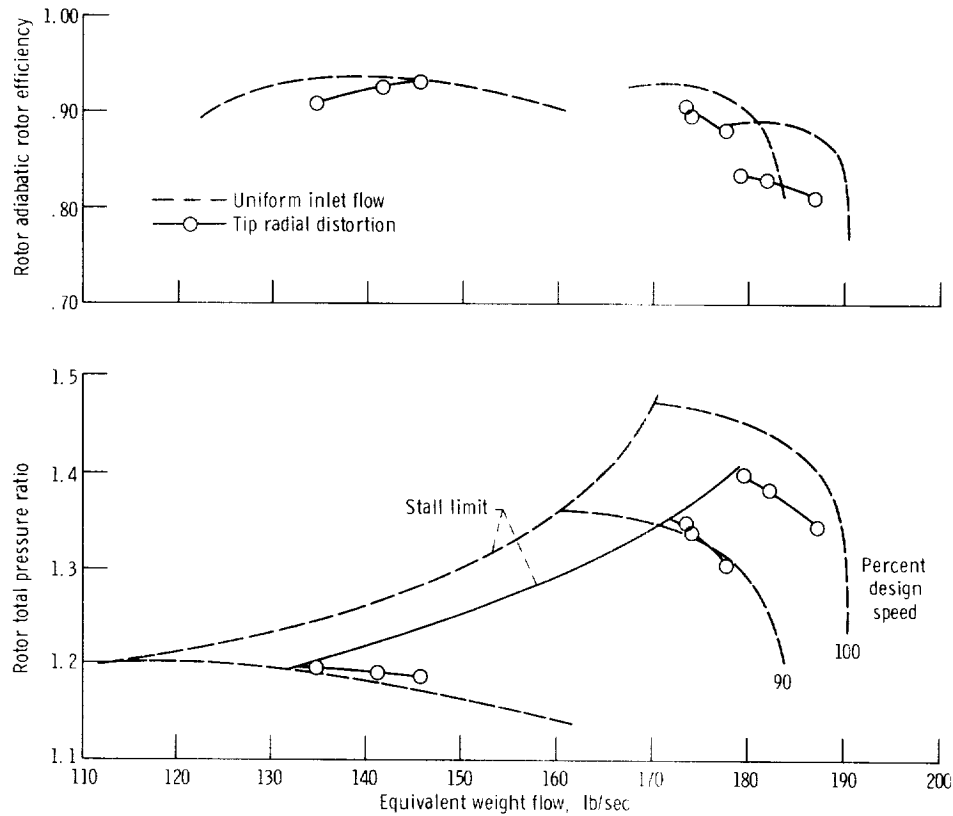


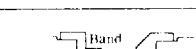
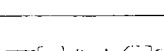
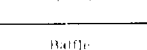
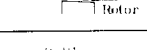
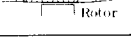
Figure 8. - Comparison of test rotor performance with tip radial distortion and uniform inlet flow for solid wall casing.

perature and pressure. This assumption, coupled with the increased radial gradients in discharge total temperature associated with a radial inlet flow distortion, introduces errors in the computed overall efficiency. Another reason for not comparing efficiencies is related to evidence of recirculatory flows in the tip region. In the presence of these recirculatory flows, there was some question of how to interpret efficiency values based on temperature measurements only.

The effectiveness of each porous casing configuration presented herein is judged primarily by a qualitative comparison of the stall limit line for the particular configuration with that for the reference (solid wall casing) configuration. Thus an improvement in the stall limit is evident when the stall limit line (on the usual pressure-ratio-against-weight-flow plot) lies to the left of the stall limit line for the reference configuration. The stall limit line is defined by the locus of flows at which rotating stall was first observed at each rotor speed studied.

In order to permit easy comparisons of the various configurations and their effects on the stall limits, a compendium is presented as table I. Each configuration is identified and a simple sketch is shown indicating the various modifications to the basic con-

TABLE I. - COMPENDIUM OF CONFIGURATIONS AND RESULTS

| Configuration number | Description | Sketch | Improvement in stall limit | Temperature in plenum less discharge total temperature measured at 10 percent passage height from tip, ΔT_p , °F | Casing static pressure 1 in. ahead of rotor leading-edge reference plane, P_1 , psia | Static pressure in plenum, P_2 , psia | Casing static pressure aft of rotor, 2.2 in. from reference plane, P_3 , psia |
|----------------------|--|---|---|--|--|---|---|
| 1 | Solid wall casing |  | Reference stall limit with tip radial distortion (fig. 8) | --- | --- | --- | --- |
| 2 | Tapered holes - open to plenum |  | Significant improvement over configuration 1 (fig. 9) | 26 | 11.8 | 13.1 | 16.1 |
| 3 | Tapered holes - all closed at plenum end |  | None | --- | --- | --- | --- |
| 4 | Tapered holes - forward two rows closed at plenum end |  | None | -24 | 11.7 | 16.0 | 16.1 |
| 5 | Tapered holes - aft row closed at plenum end |  | None | -20 | 11.8 | 11.8 | 16.2 |
| 6 | Tapered holes - forward row closed at plenum end |  | Yes, but only about one-half the amount for configuration 2 (fig. 10) | 10 | 11.9 | 14.4 | 16.4 |
| 7 | Honeycomb - full open to plenum |  | Approximately the same as for configuration 2 (fig. 11) | 82 | 12.0 | 13.9 | 16.7 |
| 8 | Honeycomb - forward portion closed at plenum end |  | Approximately the same as for configurations 2 and 7 (fig. 11) | 10 | 11.9 | 15.7 | 16.6 |
| 9 | Honeycomb - fully closed at plenum end |  | None | --- | --- | --- | --- |
| 10 | Honeycomb - configuration 8 with reduced plenum volume |  | Approximately the same as for configurations 2, 7, and 8 (fig. 12) | --- | --- | --- | --- |
| 11 | Honeycomb - configuration 10 with 36 baffles which restrict circumferential flow within plenum |  | Yes, but somewhat less than for configuration 10 (fig. 13) | --- | --- | --- | --- |
| 12 | Honeycomb - configuration 10 with baffle to restrict axial flow within plenum |  | Yes, but somewhat less than for configuration 10 (fig. 13) | --- | --- | --- | --- |
| 13 | Radial drilled holes - two rows over rotor |  | None | 20 | 11.7 | 14.6 | 16.1 |
| 14 | Radial drilled holes - two rows over rotor and two rows ahead of rotor |  | None | 64 | 11.8 | 12.3 | 16.0 |

figuration. Also included is a brief indication of the effectiveness of each configuration when tested with radial distortion.

For those configurations which showed a stall limit improvement, stall limit maps are shown in figures 9 to 13. These maps allow comparisons of the relative amounts of improvement. Figure numbers are given in table I to facilitate quick reference to these plots for a particular configuration.

Included in table I are some temperature and pressure measurements. Static pressures and temperatures were measured within the plenum when the configuration and instrument locations permitted. Also included are wall static pressures just upstream and downstream of the rotor tip. The pressures indicate the potential for recirculation, while the temperature indicates if recirculation was present. The temperature listed is the difference between the plenum temperature and the rotor discharge temperature at 10 percent passage height from the tip.

A positive temperature difference must result from some volume of air flowing forward through the plenum and receiving additional energy as it passes through the blade row again. Higher values of temperature difference indicate that this cycle is repeated numerous times. Thus, qualitatively, a higher value of temperature difference indicates increased recirculation. Negative temperature difference indicates no recirculation. Recirculatory flow rates were not measured.

No measurements were made which relate directly to the relieving of the circumferential variation in static pressure around the rotor tip. Some assessment of this possibility may be made by examining the individual sketches of table I.

Since dynamic pressure instrumentation was not used for these tests, no direct evaluation of any acoustical relations is available. Only a simple calculation of the fundamental frequency for the different passages through the casing was made. In these calculations, each passage was assumed to behave as a simple isolated organ pipe with an effective length the same as that of the passage. Because of the orientation and shape of the passages, only an approximate effective length could be determined.

Tapered holes - configurations 2 to 6. - With all the holes open at the plenum end (configuration 2), a significant stall limit improvement was obtained. The amount of the improvement as compared to the solid wall casing with tip radial distortion is shown in figure 9. The temperature and pressure data shown in table I for this configuration indicate that recirculation was present. When bands were placed over the various rows of holes at the plenum end so as to prevent recirculation (configurations 3 to 5), no stall limit improvement was noted. For configuration 6 the band located over the forward row of holes restricted but did not prevent recirculation. With this configuration a stall limit improvement was observed. However, the amount of the improvement was only approximately one-half that observed for configuration 2 where all the holes were open at the plenum end (fig. 10). The temperature values from table I indicate a lesser re-

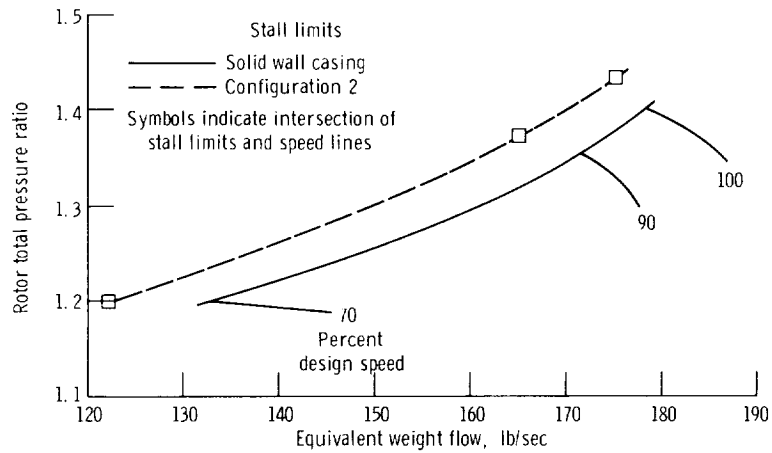


Figure 9. - Comparison of stall limits with tip radial distortion for tapered-hole configuration 2 and solid wall casing.

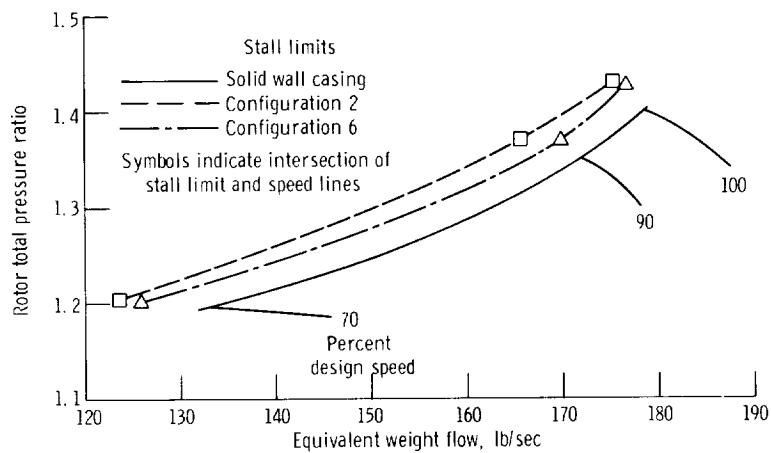


Figure 10. - Comparison of stall limits with tip radial distortion for tapered-hole configurations 2 and 6 and solid wall casing.

circulation for configuration 6 than for configuration 2. Thus, for the tapered holes, recirculation appeared to be a necessity for stall limit improvement, and the amount of the improvement was directly related to the recirculation.

From an examination of the sketches in table I, it is noted that configurations 2, 4, and 6 offer a path for the equalization of a circumferential static pressure distribution over the rotor tip. Stall limit improvements were observed for configurations 2 and 6, but not for configuration 4. From these comparisons, it appears that this mechanism was not a contributing factor for the stall limit improvement obtained with the tapered holes.

Regarding any acoustical relations, only the aft row of tapered holes, which was over the blade tip, probably needs to be considered. The fundamental frequency calculated for

the open tapered holes (configurations 2, 4, and 6) was approximately one-half the blade passing frequency at design speed. For the holes closed at the plenum end (configurations 3 and 5), a value equal to approximately 1/4 the blade passing frequency at design speed was computed. From this it appears that acoustical tuning was not a major contributing factor with the tapered holes.

Honeycomb - configurations 7 to 12. - With the honeycomb fully open over and ahead of the rotor tip (configuration 7), a significant stall limit improvement over the solid wall casing was observed (fig. 11). The amount of the improvement was approximately the same as that observed for the fully open tapered holes (configuration 2). The high temperature in the plenum indicates that recirculation is present. With a band over the forward portion of the honeycomb (configuration 8), the lower temperature shown in table I indicated less recirculation than for configuration 7. However, the stall limit improvement for configuration 8 was approximately the same as that observed for configuration 7 (fig. 11). A similar stall limit improvement with honeycomb was reported

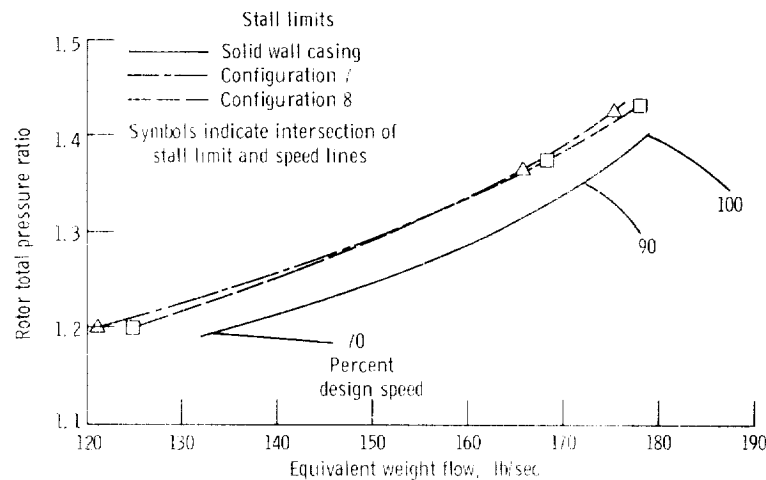


Figure 11. - Comparison of stall limits with tip radial distortion for honeycomb configurations 7 and 8 and solid wall casing.

in reference 1, with no evidence of recirculation (i. e., plenum temperature less than the discharge at 10 percent of span). From these observations, it would appear that the stall limit improvement with honeycomb was derived from different mechanisms than that for tapered holes. Some obvious differences between honeycomb and tapered holes are as follows:

(1) Directivity of recirculatory flow entering the main flow in the blade leading edge region: The compound angle of the tapered holes imparts an axial component to the returning flow. The honeycomb passages do not.

(2) Amount of open area over the blade tip: The honeycomb configuration (fig. 3) has greater open area over the blade tip than the tapered-hole configuration (fig. 4). This would allow a greater potential for equalizing the pressure field in adjacent blade passages.

(3) Recirculation: Recirculation is limited to just over the blade tip for honeycomb (configuration 8). It should be noted, however, that with a band fully covering the honeycomb (configuration 9) recirculation was zero and no improvement in stall limit was observed.

Any assessment of the honeycomb configurations with respect to equalization of static pressure around the periphery of the rotor is rather inconclusive. Configurations 7, 8, 10, and 12 offer open paths for this equalization. Configuration 9 would prevent any equalization of static pressure, and no improvement was noted.

The fundamental frequency computed for the open honeycomb passages was approximately $1\frac{1}{4}$ to $1\frac{1}{2}$ times the blade passing frequency at design speed; when the honeycomb passages were closed, the frequency was approximately one-half of this value. For those configurations showing an improvement, the amount was about the same for a range of speeds from 70 to 100 percent. If acoustical tuning is a key phenomenon, the honeycomb is not sharply tuned. However, with the honeycomb fully banded (configuration 9), acoustical tuning is the only one of the three proposed phenomena which could give an improvement and no improvement was observed.

Configurations 2 and 4 to 8 were tested with the rather large plenum which had been used for bleeding and blowing investigation as discussed in reference 1. A greatly reduced plenum volume would be desirable. Thus, configuration 8 was modified to include a band over the end flanges of the honeycomb insert. Configuration 10 represents this modification with a plenum volume less than 5 percent of the original. This configuration gave a stall limit improvement essentially equal to that for configuration 8 (see fig. 12).

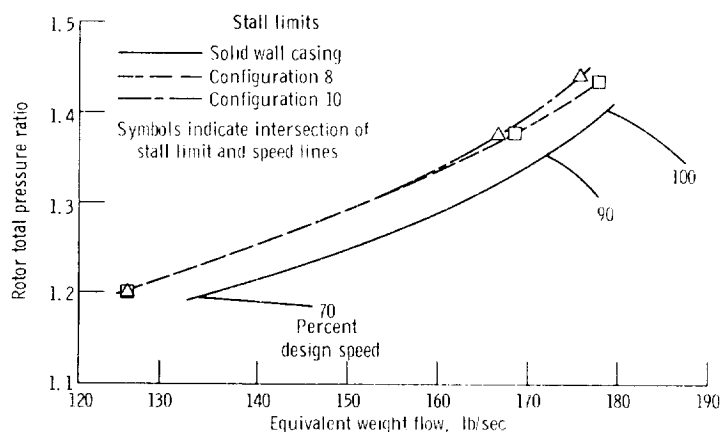


Figure 12. - Comparison of stall limits with tip radial distortion for honeycomb configurations 8 and 10 and solid wall casing.

This indicates that the size of the plenum had no effect on improvement. However, considering configuration 9, which gave no improvement, as the limiting case with zero plenum volume, then a plenum was necessary in obtaining a stall limit improvement. The preceding discussions regarding recirculation, equalization of static pressure, and acoustical tuning for configurations 7 and 8 should also hold true for configuration 10. However, no temperature or pressure measurements were made inside the small plenum. Further investigation of the effects of recirculation was made with the small plenum volume by restricting the flow within the plenum. Configuration 11 had 36 baffles approximately equally spaced around the honeycomb and oriented radially and axially. These baffles restricted the circumferential flow within the plenum. Configuration 12 had a single radial baffle around the honeycomb oriented circumferentially and located about midchord in reference to the blade tip. This baffle restricted the axial flow within the plenum. A stall limit improvement was observed for each of these configurations, but the amount of the improvement was less than that for configuration 10. These results are compared in figure 13.

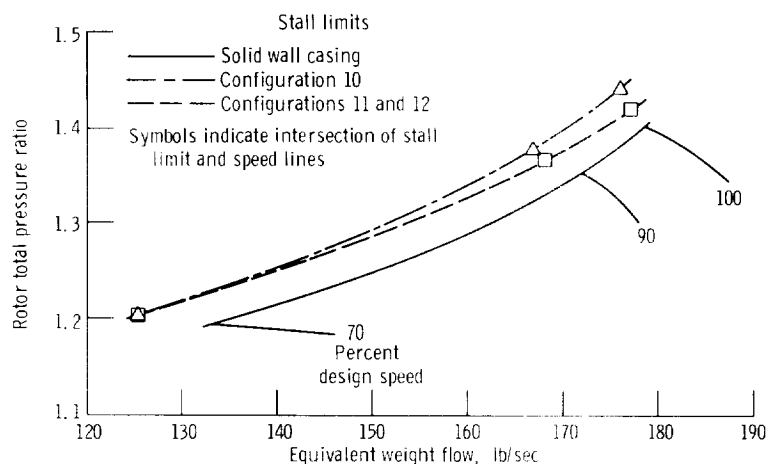


Figure 13. - Comparison of stall limits with tip radial distortion for honeycomb configurations 10, 11, and 12 and solid wall casing.

In summary, honeycomb was necessary only over the rotor tip region, a small plenum volume was adequate, and the maximum benefit was obtained when the flow within the plenum was not restricted.

Radial drilled holes - configurations 13 and 14. - No stall limit improvement was obtained with the radial drilled holes. The reason is not apparent; however, the potential for all three flow mechanisms noted with the other configuration was present: Recirculation was indicated for both configurations. Both configurations would permit equalization of the static pressure around the rotor periphery. And the fundamental

frequency computed for these holes was approximately $1\frac{1}{2}$ to $1\frac{3}{4}$ times the blade passing frequency at design speed.

Examination of the temperature data in table I indicates that with the four rows of radial drilled holes (configuration 14) the recirculation is greater than that with the tapered holes (configuration 2). One obvious difference, as with honeycomb, is that the recirculatory flow entering the main flow in the blade leading-edge region does not contain an axial component as does that for the tapered holes. The flow paths, both axially and circumferentially, for recirculation and equalization of static pressure as compared to the honeycomb configuration are apparently available, but no stall limit improvement was observed. Other differences, of course, are the amount of open area over the blade tip and the directivity of the honeycomb passages.

Even though the computed fundamental frequency for the radial drilled holes was above the blade passing frequency at design speed, none of the other configurations had indicated any narrow band tuning characteristics. Thus the radially drilled configuration, which was the most simple and easiest to build, proved to be completely ineffective.

Tests With Uniform Inlet Flow and Circumferential Distortion

The honeycomb configuration with the small plenum (configuration 10) was selected for additional testing with uniform inlet flow and circumferential inlet flow distortion. This configuration had indicated a stall limit improvement approximately equal to any porous casing configuration. The small plenum was desirable, and recirculation was probably a minimum.

Uniform inlet flow. - With uniform inlet flow, this configuration did not encounter rotating stall when it was throttled to weight flows lower than the stall limit values with the solid wall casing. Instead, the lower limit of weight flow for each speed was dictated by severe test vehicle vibrations rather than rotating stall. This vibration limit line is shown on figure 14 and compared to the stall limit line for the solid wall casing from figure 7. At weight flows somewhat higher than the vibratory limits shown on figure 14, an increase in blade stresses was noted. However, the hot-wire probes gave no indication of rotating stall.

To evaluate the effects of honeycomb casing on rotor performance, the efficiency obtained for configuration 10 with uniform inlet flow at design speed was compared to that for the solid wall casing with uniform inlet flow. Results (shown in fig. 15) indicated approximately 2 points lower overall efficiency at design speed when honeycomb casing was used. Examination of the data at the individual radial positions indicated that this lower overall efficiency was a result of the efficiency being about 8 to 9 points lower at the radial station 10 percent of span from the tip. The efficiency at the other radial

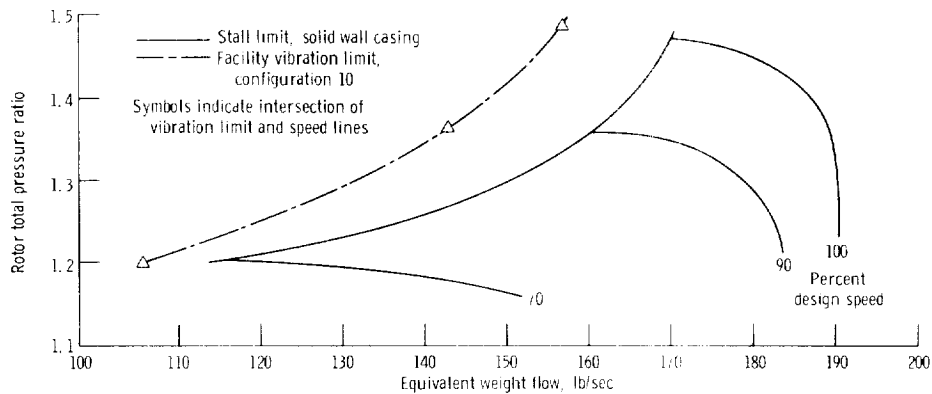


Figure 14. - Comparison of operation limits with uniform inlet flow for honeycomb configuration 10 and solid wall casing.

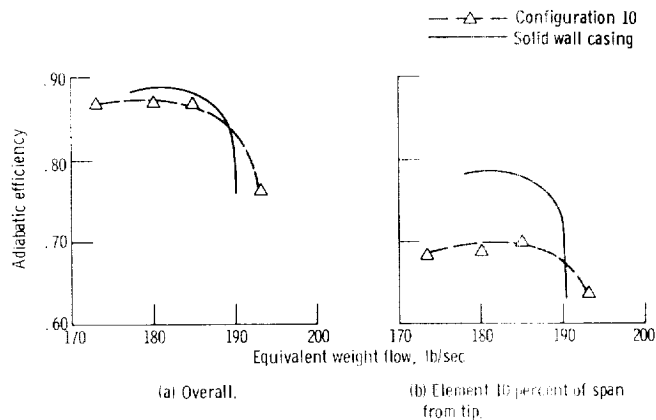


Figure 15. - Comparison of adiabatic efficiencies with uniform inlet flow for honeycomb configuration 10 and solid wall casing. Design speed.

measuring stations was approximately equal for the two configurations. This lower efficiency in the tip region was associated with a lower pressure ratio in the tip region. The temperature rise for a given radial position was about the same for both configurations, which indicates that no significant recirculation was occurring with this honeycomb configuration. However, the presence of honeycomb did change the flow in the blade tip region in such a way as to increase flow losses and decrease the pressure rise. With uniform inlet flow, the values of efficiency should be valid for the preceding comparisons.

Continuing studies have indicated that porous casing configurations can be derived which provide stall-limit improvement comparable to that shown in this investigation with little or no efficiency decrement.

Circumferential inlet flow distortion. - A significant improvement in the stall limit line was noted for configuration 10, compared to the solid wall casing, with circumfer-

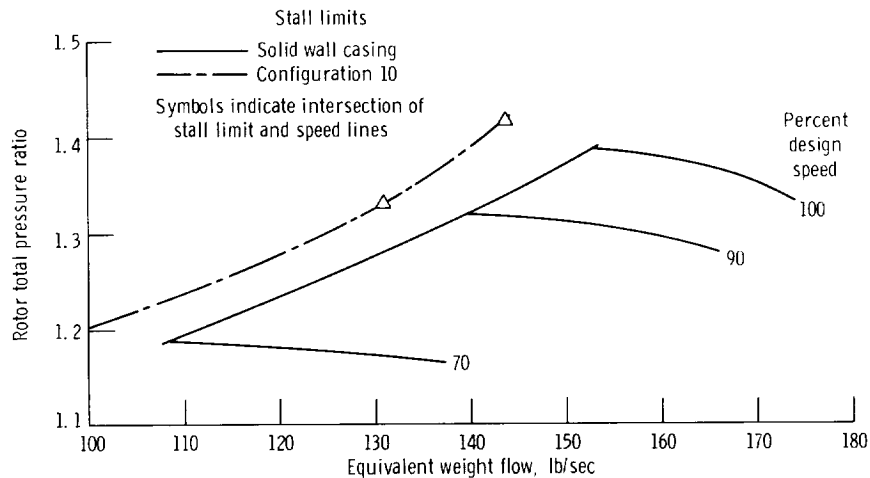


Figure 16. - Comparison of stall limits with circumferential distortion for honeycomb configuration 10 and solid wall casing. (Data for solid wall casing are from ref. 1.)

ential distortion. These results are shown in figure 16. The data for the solid wall casing with circumferential distortion were taken from reference 1.

CONCLUDING REMARKS

Limited tests have indicated that certain porous casing configurations can provide an improvement of the stall limit. Unfortunately, all the flow mechanisms and their interactions which brought about the observed improvement could not be fully identified or evaluated. Thus, it is difficult to predict how generally the results observed can be applied. The comparative results shown herein were all obtained with tip radial inlet flow distortion. Under these conditions, the tip elements of the test rotor blades were critical and tended to reach a stalling condition before the remaining blade sections. With uniform inlet flow, this rotor did not appear to be tip critical. However, the results observed are believed to be applicable to any rotor whose tip region is critical.

Two basically different porous casing configurations indicated almost identical stall limit improvements. One configuration had rows of tapered holes set at a compound angle: two rows ahead of, and the third row over, the forward part of the rotor blade tip. The second configuration had honeycomb over the rotor blade tip only and the passages tangentially inclined from the radial. With the tapered holes, there was evidence of recirculation and the amount of the improvement was directly related to the recirculation. With honeycomb, recirculation did not seem to be a controlling factor. Because of the large open area of the honeycomb casing, the stall limit improvement may be re-

lated to an ability to equalize the pressures in adjacent blade passages and thus to delay rotating stall.

The tests indicated that a plenum volume over the porous casing insert was necessary to obtain a stall limit improvement. However, tests with honeycomb indicated that a small plenum provided a stall limit improvement equal to that obtained with a larger volume. Tests with honeycomb and uniform inlet flow showed that the presence of honeycomb resulted in a reduction in rotor performance as compared with that measured with a solid wall casing. This was due primarily to a large performance loss in the rotor tip region.

A third porous casing configuration with radial drilled holes showed no stall limit improvement, although there was evidence of recirculation.

In none of the configurations tried was there any substantial evidence that acoustical tuning of the porous casing to the blade passing frequency was a significant factor in the stall limit improvement.

Further studies are required to better identify and understand the flow phenomena which are present with a porous casing, and to further explore the potential of the porous casing concept as a means of extending the operating range of compressor stages without a performance penalty.

Lewis Research Center,
National Aeronautics and Space Administration,
Cleveland, Ohio, July 13, 1970,
720-03.

APPENDIX - TABULATION OF OVERALL PERFORMANCE DATA

A tabulation of the overall performance data reported herein is given in table II. The inlet total pressure is an arithmetic average of the inlet total pressure rake measurements. In the case of radial inlet distortion, the screen covered the outer 40 percent of the annulus area and two of the five elements in each rake were behind the screen. For circumferential distortion, the screen covered one-fourth of the circumferential inlet area (90° segment) and one of the four rakes was behind the screen. Hence, an arithmetic average is considered to be adequate. For the discharge total pressures and temperatures, the measurements were arithmetically averaged at each radial measuring position, and were then mass averaged radially. The measured total pressure, total temperature, and a linear variation of static pressure from hub to tip were used for the mass averaging.

The last three values of corrected weight flow and speed listed for each configuration are the weight flows at the stall points for the three speeds tested.

TABLE II - OVERALL PERFORMANCE^a

| Reading | Pressure ratio | Corrected efficiency, percent | Total corrected flow, lb sec | Bellmouth flow, lb sec | Average total inlet pressure, psia | Average inlet temperature, °R | Corrected speed, percent |
|--|----------------|-------------------------------|------------------------------|------------------------|------------------------------------|-------------------------------|--------------------------|
| Solid wall casing with uniform inlet flow | | | | | | | |
| 1 | 1.140 | 0.958 | ---- | 159.40 | 14.83 | 505.3 | 70.0 |
| 2 | 1.139 | .901 | 160.82 | 159.46 | 14.74 | 512.1 | 70.1 |
| 3 | 1.200 | .893 | 122.14 | 120.59 | 14.76 | 519.3 | 70.0 |
| 4 | 1.208 | .817 | 183.55 | 183.61 | 14.72 | 519.0 | 90.1 |
| 5 | 1.354 | .924 | 167.43 | 166.50 | 14.74 | 509.5 | 90.0 |
| 6 | 1.233 | .769 | 190.22 | 190.37 | 14.71 | 508.7 | 100.1 |
| 7 | 1.457 | .888 | 177.82 | 176.39 | 14.72 | 508.5 | |
| 8 | 1.395 | .875 | 187.42 | 186.12 | 14.70 | 508.1 | |
| 9 | 1.350 | .851 | 189.68 | 188.88 | | 508.2 | |
| 10 | 1.269 | .878 | ----- | 181.52 | | 508.0 | 90.0 |
| 11 | 1.308 | .913 | 178.48 | 177.18 | | 507.5 | 90.0 |
| 12 | 1.181 | .935 | 140.75 | 138.94 | 14.73 | 507.6 | 70.0 |
| --- | ----- | ----- | 113 | ----- | ----- | ----- | 70 |
| --- | ----- | ----- | 160 | ----- | ----- | ----- | 90 |
| --- | ----- | ----- | 170 | ----- | ----- | ----- | 100 |
| Solid wall casing with tip radial distortion | | | | | | | |
| 19 | 1.188 | 0.936 | 145.44 | 144.13 | 12.95 | 523.8 | 70.0 |
| 20 | 1.196 | .908 | 134.64 | 132.03 | 13.99 | 509.4 | 70.0 |
| 21 | 1.307 | .883 | 177.56 | 177.33 | 13.09 | 509.2 | 90.1 |
| 22 | 1.350 | .907 | 173.26 | 172.89 | 13.20 | 508.5 | 90.0 |
| 23 | 1.345 | .813 | 186.89 | 183.53 | 12.92 | 508.0 | 100.1 |
| 24 | 1.399 | .836 | 179.08 | 178.55 | 13.07 | 507.8 | 100.1 |
| 25 | 1.383 | .831 | 181.77 | 180.49 | 13.02 | 507.0 | 100.1 |
| 26 | 1.339 | .895 | 173.77 | 174.47 | 13.19 | 508.1 | 90.2 |
| 27 | 1.191 | .923 | 140.96 | 139.76 | 13.90 | 505.3 | 70.0 |
| --- | ----- | ----- | 132 | ----- | ----- | ----- | 70 |
| --- | ----- | ----- | 170 | ----- | ----- | ----- | 90 |
| --- | ----- | ----- | 179 | ----- | ----- | ----- | 100 |
| Radial drilled holes - configuration 13 with tip radial distortion | | | | | | | |
| 28 | 1.188 | 0.936 | 145.69 | 144.09 | 13.82 | 517.4 | 70.0 |
| 29 | 1.196 | .911 | 134.29 | 132.47 | 14.00 | 517.9 | 70.0 |
| 30 | 1.192 | .912 | 139.23 | 138.40 | 13.91 | 516.1 | 70.1 |
| 31 | 1.306 | .877 | 179.22 | 177.02 | 13.11 | 517.2 | 90.1 |
| 32 | 1.360 | .904 | 171.55 | 169.40 | 13.31 | 517.6 | 90.0 |
| 33 | 1.347 | .910 | 174.53 | 173.15 | 13.22 | 517.0 | 90.1 |
| 34 | 1.346 | .811 | 185.56 | 183.53 | 12.92 | 516.6 | 100.1 |
| 35 | 1.407 | .837 | 180.60 | 178.08 | 13.09 | 513.1 | 100.2 |
| 36 | 1.384 | .837 | 182.06 | 180.76 | 13.01 | 516.7 | 99.8 |
| 37 | 1.402 | .847 | 181.80 | 179.87 | 13.02 | 517.4 | 100.0 |
| --- | ----- | ----- | 132 | ----- | ----- | ----- | 70 |
| --- | ----- | ----- | 170 | ----- | ----- | ----- | 90 |
| --- | ----- | ----- | 180 | ----- | ----- | ----- | 100 |
| Radial drilled holes - configuration 14 with tip radial distortion | | | | | | | |
| 38 | 1.186 | 0.903 | 144.87 | 143.21 | 13.87 | 517.9 | 70.1 |
| 39 | 1.196 | .879 | 127.66 | 125.74 | 14.12 | 521.8 | 69.9 |
| 40 | 1.194 | .920 | 135.99 | 134.35 | 14.00 | 520.0 | 70.1 |
| 41 | 1.302 | .868 | 177.29 | 175.82 | 13.17 | 519.6 | 90.0 |
| 42 | 1.343 | .908 | 172.33 | 170.50 | 13.30 | 521.8 | 90.0 |
| 43 | 1.329 | .867 | 175.35 | 173.44 | 13.22 | 523.5 | 90.0 |
| 44 | 1.342 | .802 | 184.58 | 182.62 | 12.96 | 523.0 | 100.1 |
| 45 | 1.396 | .832 | 180.04 | 177.53 | 13.11 | 523.3 | 100.1 |
| 46 | 1.374 | .827 | 182.08 | 180.18 | 13.03 | 523.7 | 100.0 |
| --- | ----- | ----- | 125 | ----- | ----- | ----- | 70 |
| --- | ----- | ----- | 171 | ----- | ----- | ----- | 90 |
| --- | ----- | ----- | 179 | ----- | ----- | ----- | 100 |

^aTabulation from computer output.

TABLE II. - Continued. OVERALL PERFORMANCE³

| Reading | Pressure ratio | Corrected efficiency, percent | Total corrected flow, lb/sec | Bellmouth flow, lb/sec | Average total inlet pressure, psia | Average inlet temperature, °R | Corrected speed, percent |
|--|----------------|-------------------------------|------------------------------|------------------------|------------------------------------|-------------------------------|--------------------------|
| Tapered holes - configuration 2 with tip radial distortion | | | | | | | |
| 47 | 1.190 | 0.947 | 143.70 | 143.69 | 13.64 | 508.2 | 70.0 |
| 48 | 1.201 | .908 | 125.37 | 125.31 | 13.92 | 509.0 | 70.1 |
| 49 | 1.200 | .927 | 134.61 | 133.05 | 13.81 | 509.0 | 70.1 |
| 50 | 1.308 | .881 | 177.39 | 176.38 | 12.93 | 507.8 | 90.1 |
| 51 | 1.368 | .917 | 167.03 | 166.69 | 13.17 | 507.7 | 90.0 |
| 52 | 1.356 | .925 | 172.65 | 171.41 | 13.05 | 508.0 | 90.1 |
| 53 | 1.347 | .820 | 183.35 | 182.43 | 12.73 | 508.1 | 100.0 |
| 54 | 1.416 | .858 | 177.61 | 176.15 | 12.91 | 508.1 | 100.0 |
| 55 | 1.403 | .848 | 178.79 | 178.07 | 12.86 | 507.3 | 100.0 |
| 56 | 1.394 | .846 | 178.43 | 179.30 | 12.82 | 507.3 | 100.1 |
| --- | --- | --- | 123 | --- | --- | --- | 70 |
| --- | --- | --- | 165 | --- | --- | --- | 90 |
| --- | --- | --- | 174 | --- | --- | --- | 100 |
| Tapered holes - configuration 3 with tip radial distortion | | | | | | | |
| 57 | 1.350 | 0.826 | 183.52 | 182.97 | 12.66 | 504.7 | 100.0 |
| 58 | 1.424 | .888 | 180.67 | 179.58 | 12.67 | 505.0 | 100.0 |
| 59 | 1.395 | .850 | 179.88 | 178.80 | 12.78 | 505.2 | 100.0 |
| 60 | 1.303 | .875 | 175.92 | 176.27 | 12.84 | 505.3 | 90.1 |
| 61 | 1.336 | .909 | 173.84 | 174.01 | 12.89 | 505.5 | 90.0 |
| 62 | 1.357 | .930 | 171.41 | 170.26 | 12.99 | 505.8 | 90.0 |
| 63 | 1.191 | .953 | 144.06 | 143.51 | 13.54 | 505.7 | 70.0 |
| 64 | 1.196 | .915 | 131.09 | 130.95 | 13.73 | 505.7 | 70.0 |
| 65 | 1.195 | .935 | 136.91 | 136.54 | 13.64 | 505.6 | 70.0 |
| --- | --- | --- | 130 | --- | --- | --- | 70 |
| --- | --- | --- | 170 | --- | --- | --- | 90 |
| --- | --- | --- | 179 | --- | --- | --- | 100 |
| Tapered holes - configuration 4 with tip radial distortion | | | | | | | |
| 66 | 1.191 | 0.955 | 144.12 | 143.53 | 13.51 | 510.4 | 70.0 |
| 67 | 1.190 | .952 | 144.46 | 143.55 | 13.51 | 511.0 | ↓ |
| 68 | 1.199 | .917 | 131.94 | 130.97 | 13.71 | 511.5 | |
| 69 | 1.195 | .948 | 139.50 | 137.73 | 13.61 | 511.3 | ↓ |
| 70 | 1.312 | .889 | 176.90 | 176.51 | 12.77 | 514.1 | |
| 71 | 1.358 | .913 | 172.96 | 171.37 | 12.93 | 513.9 | 90.0 |
| 72 | 1.340 | .901 | 175.67 | 174.76 | 12.85 | 514.1 | 90.0 |
| 73 | 1.352 | .820 | 185.25 | 183.40 | 12.60 | 513.1 | 100.1 |
| 74 | 1.409 | .853 | 180.64 | 178.46 | 12.75 | 512.2 | 100.1 |
| 75 | 1.396 | .842 | 181.39 | 180.28 | 12.70 | 512.6 | 100.0 |
| --- | --- | --- | 131 | --- | --- | --- | 70 |
| --- | --- | --- | 172 | --- | --- | --- | 90 |
| --- | --- | --- | 180 | --- | --- | --- | 100 |
| Tapered holes - configuration 6 with tip radial distortion | | | | | | | |
| 76 | 1.348 | 0.813 | 184.60 | 183.76 | 12.62 | 514.0 | 100.0 |
| 77 | 1.422 | .854 | 177.19 | 176.43 | 12.83 | 511.4 | 100.1 |
| 78 | 1.404 | .850 | 181.26 | 178.76 | 12.76 | 511.9 | 99.8 |
| 79 | 1.309 | .891 | 176.24 | 176.40 | 12.82 | 507.8 | 90.0 |
| 80 | 1.367 | .922 | 170.49 | 167.87 | 13.04 | 506.1 | 90.1 |
| 81 | 1.355 | .924 | 173.23 | 171.24 | 12.94 | 505.0 | 90.0 |
| 82 | 1.191 | .952 | 145.18 | 143.51 | 13.52 | 505.1 | 70.0 |
| 83 | 1.201 | .902 | 127.24 | 126.93 | 13.77 | 504.5 | 70.0 |
| 84 | 1.198 | .922 | 136.82 | 133.99 | 13.67 | 504.1 | 70.1 |
| --- | --- | --- | 126 | --- | --- | --- | 70 |
| --- | --- | --- | 170 | --- | --- | --- | 90 |
| --- | --- | --- | 176 | --- | --- | --- | 100 |

³Tabulation from computer output.

TABLE II. - Continued. OVERALL PERFORMANCE^a

| Reading | Pressure ratio | Corrected efficiency, percent | Total corrected flow, lb/sec | Bellmouth flow, lb/sec | Average total inlet pressure, psia | Average inlet temperature, °R | Corrected speed, percent |
|--|----------------|-------------------------------|------------------------------|------------------------|------------------------------------|-------------------------------|--------------------------|
| Tapered holes - configuration 5 with tip radial distortion | | | | | | | |
| 85 | 1.353 | 0.828 | 186.00 | 184.03 | 12.59 | 503.9 | 100.0 |
| 86 | 1.390 | .849 | 182.58 | 181.55 | 12.66 | 504.0 | ↓ |
| 87 | 1.412 | .858 | 179.96 | 178.65 | 12.75 | 504.2 | |
| 88 | 1.399 | .841 | 182.40 | 179.90 | 12.71 | 504.2 | 90.0 |
| 89 | 1.312 | .905 | 178.37 | 177.02 | 12.79 | 504.3 | |
| 90 | 1.361 | .925 | 172.23 | 171.16 | 12.96 | 503.9 | 90.0 |
| 91 | 1.345 | .912 | 174.82 | 174.03 | 12.87 | 503.8 | 90.0 |
| 92 | 1.193 | .949 | 146.71 | 143.82 | 13.54 | 503.8 | 70.0 |
| 93 | 1.195 | .907 | 133.22 | 131.54 | 13.74 | 503.7 | ↓ |
| 94 | 1.198 | .942 | 138.30 | 137.09 | 13.66 | 503.8 | |
| --- | --- | --- | 131 | --- | --- | --- | 90 |
| --- | --- | --- | 173 | --- | --- | --- | |
| --- | --- | --- | 180 | --- | --- | --- | 100 |
| Honeycomb - configuration 8 with tip radial distortion | | | | | | | |
| 95 | 1.190 | 0.954 | 144.01 | 144.55 | 13.75 | 530.1 | 69.9 |
| 96 | 1.200 | .911 | 127.55 | 126.89 | 14.01 | 530.1 | 70.0 |
| 97 | 1.198 | .936 | 135.47 | 134.97 | 13.89 | 530.5 | 70.0 |
| 98 | 1.313 | .901 | 178.41 | 177.36 | 12.97 | 531.4 | 89.9 |
| 99 | 1.372 | .932 | 168.29 | 167.14 | 13.25 | 532.0 | 90.0 |
| 100 | 1.368 | .933 | 172.20 | 171.15 | 13.14 | 531.4 | 90.0 |
| 101 | 1.354 | .827 | 186.53 | 184.54 | 12.75 | 531.9 | 100.0 |
| 102 | 1.429 | .866 | 178.68 | 177.55 | 12.97 | 531.9 | 100.0 |
| 103 | 1.412 | .857 | 181.46 | 179.99 | 12.89 | 530.3 | 100.1 |
| --- | --- | --- | 126 | --- | --- | --- | 70 |
| --- | --- | --- | 167 | --- | --- | --- | 90 |
| --- | --- | --- | 178 | --- | --- | --- | 100 |
| Honeycomb - configuration 7 with radial tip distortion | | | | | | | |
| 104 | 1.191 | 0.954 | 144.98 | 143.57 | 13.71 | 528.1 | 70.0 |
| 105 | 1.201 | .917 | 121.04 | 119.64 | 14.07 | 526.6 | 70.0 |
| 106 | 1.200 | .923 | 131.59 | 130.87 | 13.91 | 525.9 | 70.1 |
| 107 | 1.308 | .891 | 176.95 | 175.83 | 12.97 | 526.3 | 90.0 |
| 108 | 1.365 | .933 | 166.08 | 165.91 | 13.24 | 527.2 | ↓ |
| 109 | 1.364 | .933 | 167.17 | 166.55 | 13.22 | 527.2 | |
| 110 | 1.356 | .928 | 170.77 | 169.69 | 13.13 | 526.9 | 100.0 |
| 111 | 1.346 | .823 | 182.96 | 182.41 | 12.77 | 526.8 | |
| 112 | 1.421 | .865 | 176.95 | 175.62 | 12.96 | 526.7 | 100.0 |
| 113 | 1.411 | .860 | 177.29 | 177.41 | 12.92 | 526.7 | 99.9 |
| 114 | 1.394 | .848 | 179.09 | 178.92 | 12.86 | 526.8 | 99.9 |
| --- | --- | --- | 120 | --- | --- | --- | 70 |
| --- | --- | --- | 164 | --- | --- | --- | 90 |
| --- | --- | --- | 175 | --- | --- | --- | 100 |
| Honeycomb - configuration 10 with tip radial distortion | | | | | | | |
| 115 | 1.354 | 0.832 | 183.91 | 184.19 | 12.63 | 525.2 | 100.0 |
| 116 | 1.427 | .882 | 178.19 | 177.34 | 12.83 | 524.7 | ↓ |
| 117 | 1.421 | .873 | 180.80 | 179.41 | 12.75 | 524.2 | |
| 118 | 1.406 | .868 | 180.47 | 180.47 | 12.74 | 523.3 | 89.9 |
| 119 | 1.311 | .899 | 177.50 | 176.77 | 12.85 | 523.6 | |
| 120 | 1.370 | .966 | 168.53 | 167.46 | 13.10 | 523.4 | 90.0 |
| 121 | 1.351 | .919 | 171.16 | 171.12 | 13.01 | 523.7 | 89.9 |
| 122 | 1.193 | .947 | 143.95 | 143.55 | 13.60 | 523.7 | 69.9 |
| 123 | 1.200 | .929 | 127.59 | 126.93 | 13.87 | 523.9 | 69.9 |
| 124 | 1.199 | .940 | 134.56 | 134.54 | 13.76 | 524.0 | 69.9 |
| --- | --- | --- | 125 | --- | --- | --- | 70 |
| --- | --- | --- | 166 | --- | --- | --- | 90 |
| --- | --- | --- | 175 | --- | --- | --- | 100 |

^aTabulation from computer output.

TABLE II. - Concluded. OVERALL PERFORMANCE^a

| Reading | Pressure ratio | Corrected efficiency, percent | Total corrected flow, lb/sec | Bellmouth flow, lb/sec | Average total inlet pressure, psia | Average inlet temperature, °R | Corrected speed, percent |
|--|----------------|-------------------------------|------------------------------|------------------------|------------------------------------|-------------------------------|--------------------------|
| Honeycomb - configuration 9 with tip radial distortion | | | | | | | |
| 125 | 1.358 | 0.830 | 185.28 | 185.31 | 12.77 | 517.0 | 100.1 |
| 126 | 1.411 | .857 | 180.63 | 178.56 | 12.99 | 516.7 | 99.9 |
| 127 | 1.495 | .832 | 181.69 | 179.44 | 12.96 | 515.9 | 100.0 |
| 128 | 1.390 | .843 | 180.73 | 181.71 | 12.85 | 516.5 | 99.9 |
| 129 | 1.315 | .897 | 178.67 | 177.56 | 13.01 | 515.9 | 89.9 |
| 130 | 1.355 | .917 | 173.20 | 171.98 | 13.16 | 515.3 | 90.0 |
| 131 | 1.340 | .897 | 175.69 | 174.24 | 13.10 | 514.8 | 90.0 |
| 132 | 1.193 | .943 | 144.38 | 143.34 | 13.78 | 515.1 | 69.9 |
| 133 | 1.199 | .919 | 130.02 | 130.34 | 13.99 | 514.5 | 70.0 |
| 134 | 1.197 | .928 | 137.21 | 135.81 | 13.91 | 514.8 | 69.9 |
| --- | --- | --- | 129 | --- | --- | --- | 70 |
| --- | --- | --- | 173 | --- | --- | --- | 90 |
| --- | --- | --- | 180 | --- | --- | --- | 100 |
| Honeycomb - configuration 11 with tip radial distortion | | | | | | | |
| 135 | 1.353 | 0.823 | 184.92 | 183.46 | 12.83 | 513.7 | 100.0 |
| 136 | 1.419 | .858 | 179.24 | 176.63 | 13.04 | 514.2 | 100.0 |
| 137 | 1.413 | .851 | 179.21 | 177.94 | 12.99 | 514.0 | 99.9 |
| 138 | 1.401 | .847 | 181.35 | 179.58 | 12.94 | 514.2 | 99.9 |
| 139 | 1.306 | .870 | 177.43 | 176.62 | 13.02 | 513.4 | 90.0 |
| 140 | 1.366 | .920 | 169.37 | 168.19 | 13.26 | 513.1 | 90.0 |
| 141 | 1.353 | .906 | 173.22 | 172.18 | 13.15 | 512.9 | 90.0 |
| 142 | 1.192 | .933 | 145.08 | 143.23 | 13.78 | 512.4 | 70.0 |
| 143 | 1.198 | .896 | 128.17 | 126.72 | 14.05 | 513.0 | 69.9 |
| 144 | 1.198 | .916 | 136.51 | 135.09 | 13.92 | 512.9 | 69.9 |
| 145 | 1.417 | .851 | 177.44 | 176.94 | 13.03 | 513.2 | 99.9 |
| --- | --- | --- | 127 | --- | --- | --- | 70 |
| --- | --- | --- | 168 | --- | --- | --- | 90 |
| --- | --- | --- | 177 | --- | --- | --- | 100 |
| Honeycomb - configuration 12 with tip radial distortion | | | | | | | |
| 146 | 1.359 | 0.838 | 185.13 | 185.20 | 12.76 | 524.7 | 100.0 |
| 147 | 1.414 | .847 | 179.30 | 178.63 | 12.96 | 524.1 | 100.0 |
| 148 | 1.404 | .841 | 180.67 | 180.48 | 12.90 | 518.6 | 100.1 |
| 149 | 1.399 | .845 | 182.69 | 182.04 | 12.82 | 517.8 | 99.9 |
| 150 | 1.316 | .888 | 178.47 | 177.62 | 12.97 | 516.6 | 90.0 |
| 151 | 1.361 | .918 | 171.11 | 170.56 | 13.17 | 515.4 | 90.0 |
| 152 | 1.354 | .914 | 173.51 | 172.98 | 13.10 | 516.2 | 89.9 |
| 153 | 1.193 | .946 | 143.99 | 143.76 | 13.74 | 516.0 | 69.9 |
| 154 | 1.202 | .926 | 130.15 | 129.04 | 13.94 | 515.7 | 69.9 |
| 155 | 1.199 | .920 | 136.69 | 136.02 | 13.86 | 515.5 | 70.0 |
| --- | --- | --- | 127 | --- | --- | --- | 70 |
| --- | --- | --- | 169 | --- | --- | --- | 90 |
| --- | --- | --- | 178 | --- | --- | --- | 100 |
| Honeycomb - configuration 10 with circumferential distortion | | | | | | | |
| 156 | 1.169 | 0.900 | 138.95 | 139.94 | 14.10 | 516.8 | 69.8 |
| 157 | 1.194 | .755 | 102.64 | 101.98 | 14.46 | 518.1 | 69.9 |
| 158 | 1.189 | .798 | 116.00 | 115.40 | 14.35 | 517.7 | 69.9 |
| 159 | 1.347 | .808 | 179.71 | 178.96 | 13.38 | 518.7 | 99.8 |
| 160 | 1.411 | .733 | 148.42 | 148.35 | 13.90 | 518.3 | 100.0 |
| 161 | 1.404 | .744 | 158.31 | 157.04 | 13.78 | 520.5 | 99.9 |
| 162 | 1.392 | .747 | 165.27 | 163.51 | 13.69 | 521.0 | 99.8 |
| 163 | 1.286 | .864 | 169.92 | 169.49 | 13.59 | 520.3 | 90.0 |
| 164 | 1.330 | .753 | 136.09 | 135.46 | 14.09 | 520.9 | 89.9 |
| 165 | 1.325 | .795 | 152.98 | 152.61 | 13.87 | 519.1 | 90.2 |
| --- | --- | --- | 98 | --- | --- | --- | 70 |
| --- | --- | --- | 131 | --- | --- | --- | 90 |
| --- | --- | --- | 144 | --- | --- | --- | 100 |
| Honeycomb - configuration 10 with uniform inlet flow | | | | | | | |
| 166 | 1.232 | 0.763 | 192.91 | 191.55 | 14.65 | 529.0 | 100.0 |
| 167 | 1.460 | .868 | 173.23 | 171.72 | 14.66 | 528.7 | ↓ |
| 168 | 1.431 | .872 | 179.99 | 179.67 | 14.66 | 528.7 | ↓ |
| 169 | 1.399 | .869 | 184.87 | 183.90 | 14.66 | 528.9 | ↓ |
| 170 | 1.209 | .830 | 185.64 | 184.64 | 14.65 | 529.2 | 90.0 |
| 171 | 1.351 | .914 | 166.13 | 165.68 | 14.68 | 528.3 | 90.1 |
| 172 | 1.304 | .915 | 178.27 | 176.54 | 14.67 | 527.2 | 90.1 |
| 173 | 1.139 | .931 | 160.75 | 159.44 | 14.68 | 527.0 | 70.0 |
| 174 | 1.198 | .866 | 119.60 | 117.84 | 14.72 | 525.5 | 70.1 |
| 175 | 1.176 | .917 | 141.68 | 140.27 | 14.71 | 522.4 | 70.2 |
| 176 | 1.177 | .943 | 140.55 | 140.75 | 14.70 | 522.3 | 70.2 |
| --- | --- | --- | ^b 105 | --- | --- | --- | 70 |
| --- | --- | --- | ^b 142 | --- | --- | --- | 90 |
| --- | --- | --- | ^b 156 | --- | --- | --- | 100 |

^aTabulation from computer output.

^bFacility vibration limit, with no rotating stall.

REFERENCES

1. Koch, C. C. : Experimental Evaluation of Outer Case Blowing or Bleeding of Single Stage Axial Flow Compressor. Part VI: Final Report. Rep. R69AEG256, General Electric Co. (NASA CR-54592), Jan. 30, 1970.
2. Giffin, R. G. ; and Smith, L. H. , Jr. : Experimental Evaluation of Outer Case Blowing or Bleeding of Single Stage Axial Flow Compressor. Part I: Design of Rotor and Bleeding and Blowing Configurations. Rep. R66FPD137, General Electric Co. (NASA CR-54587), Apr. 20, 1966.
3. Koch, C. C. ; and Smith, L. H. , Jr. : Experimental Evaluation of Outer Case Blowing or Bleeding of Single Stage Axial Flow Compressor. Part III: Performance of Blowing Insert Configuration No. 1. Rep. R68AEG318, General Electric Co. (NASA CR-54589), Nov. 22, 1968.
4. Koch, C. C. ; and Smith, L. H. , Jr. : Experimental Evaluation of Outer Case Blowing or Bleeding of Single Stage Axial Flow Compressor. Part IV: Performance of Bleed Insert Configuration No. 3. Rep. R68AEG357, General Electric Co. (NASA CR-54590), Aug. 29, 1968.